PRODUCTION OF CERAMIC COATINGS ON AA6061 ALUMINUM ALLOY USING PLASMA ELECTROLYTIC OXIDATION

V. Dehnavi[1], B. Luan[2,3], X.Y. Liu[2], D. W. Shoesmith[3,4], S. Rohani[1]

[1]Department of Chemical and Biochemical Engineering, University of Western Ontario, London, ON, N6A 5B9, Canada.
[2]National Research Council Canada, 800 Collip Circle, London, ON, N6G 4X8, Canada
[3]Department of Chemistry, University of Western Ontario, London, ON, N6A 5B7, Canada
[4]Surface Science Western, 999 Collip Circle, London, ON, N6G 0J3, Canada

Keywords: Plasma Electrolytic Oxidation, Aluminum Alloy 6061, Ceramic Coatings

Abstract:

Plasma electrolytic oxidation (PEO) is a relatively novel surface finishing technique that converts the surface of light metals and alloys into oxide layers. For Al alloys, the coatings produced by PEO mainly consist of oxides with high hardness and therefore are more suitable for tribological applications than the substrate material. The PEO coatings can also effectively protect the base metal against corrosion. In this study ceramic coatings were deposited on 6061 Al alloy substrates using an alkaline electrolyte. The morphology, microstructure, compositions, and growth behavior of the coatings were analyzed using SEM, energy-dispersive X-ray spectroscopy (EDX), and X-ray diffraction (XRD). The results suggest that the coating growth behavior is a function of the PEO process stages. This information can be used to better understand the PEO coating growth behavior and to improve the quality of the coatings for required applications.

Introduction

Plasma electrolytic oxidation (PEO), which is a relatively novel surface modification technique, has attracted a lot of interest as an effective method to produce coatings with improved hardness, wear and corrosion resistance on the surface of aluminum alloys [1, 2]. PEO is a plasma-assisted electrochemical surface treatment which operates at high electrical potentials, typically several hundred volts. At potentials greater than the breakdown voltage of the oxide film, a large number of short-lived micro-discharges are formed which create the oxide layer [3, 4]. The structure of the oxide ceramic coatings resembles sintered oxide ceramics and their formation is the result of the local thermal action of the sparks [5]. As the oxide layer grows and thickens, the micro-discharges developing on the sample surface become more intense which can result in detrimental defects in the oxide layer [6].

Aqueous solutions containing silicates can passivate the surface of the aluminum substrate and are considered as one of the most suitable electrolytes for the PEO process. These alkaline electrolytes are environmentally friendly and as a result PEO is attracting growing interests in many industries including transport, energy and medicine. PEO is a good substitute for conventional and hard anodizing methods in which acidic electrolytes containing chrome are used which create severe pollution and environmental issues [4, 7, 8].

Despite various investigations conducted by many researchers, the PEO coatings formation mechanism is still not fully understood [9, 10]. Typically four stages are distinguished in the PEO process [8, 11]. The phenomenon and mechanism happening in each stage and the resulting effects on the oxide layer growth behaviour are different. Applied process parameters can change the duration and ratio of these stages. Investigating the correlation between coating characteristics and different stages of PEO can improve the understanding of the process. In the present study, aluminum substrates were PEO coated in an electrolyte containing a relatively high concentration (10 g/L) of sodium silicate. Samples were coated at different treatment times and particular attention was paid to correlate the voltage-time responses of the PEO coating process and the oxide layer characteristics so as to understand the coating growth behavior during different stages of PEO.

Experimental Procedure

Disk samples with a diameter of about 3 cm and a thickness of 7-9 mm were cut from a 6061-T651 aluminum alloy bar supplied by Kaiser Aluminum, USA. To ensure a reproducible initial surface condition, samples were polished with 600 grit emery polishing paper followed by degreasing in propanol and rinsing with distilled water. A PEO unit custom-built by National Research Council Canada equipped with a DC power supply was used to produce the coatings. The positive output of the power supply was connected to the sample immersed in the electrolyte serving as the working electrode (anode) and the negative output was connected to the stainless steel electrolyte container acting as the counter electrode (cathode). To ensure a good connection between the power supply and the samples, a threaded hole was drilled on one side of each sample. Then the sample was bolted to a steel rod (insulated by a ceramic jacket from the electrolyte) connected to the power supply. PEO coatings were produced using the uni-polar pulsed DC mode with a square waveform applied at a frequency of 900 Hz. Samples were coated at a duty cycle (D_t) of 20%. The duty cycle is defined as:

$$D_t = [\ t_{on} / (t_{on} + t_{off})] \times 100 \qquad (1)$$

where t_{on} is the 'on' duration and t_{off} is the 'off' duration during a single cycle. The PEO process was carried out at a constant current density of 1000 A/m^2. Table I lists the sample codes and deposition times.

Table I – Sample codes and deposition times

Sample code	Deposition time (min)
S1	10
S2	20
S4	40
S6	60

The electrolyte was a solution of 10 g/L Na_2SiO_3 and 0.5 g/L KOH in deionized water. The electrolyte temperature was maintained below 30 °C during treatment using an external DCA 500 Durachill heat exchanger manufactured by Polyscience.

Coating thickness was evaluated using an Eddy current gauge. Ten measurements were taken on the coated surface of each sample. Statistical treatments were applied to extract the mean data values and scatter. Coating surfaces and cross sections were examined using a LEO 440 scanning electron microscope (SEM) equipped with a Quartz EDX system and a Hitachi S-3500N SEM equipped with an Oxford Instruments 7490 X-ray detector. The samples were sputter-coated with gold prior to SEM imaging to minimize surface charging. A Philips X'Pert_MRD diffractometer with Cu K_α (40 kV and 40 mA) radiation was used to study the phase composition of the coatings. The samples were scanned in the 2θ range from 20° to 100° with a 0.02 ° step size.

Results and Discussion

1-Voltage-Time Response during PEO Treatment

The voltage-time curve of the PEO coating process of the sample treated for 60 min is presented in Figure 1. Since voltage-time curves of other samples coated at shorter times overlapped, only one curve is illustrated. Generally four different stages are believed to take place during PEO [8, 11]. During the first stage, as the applied voltage increases, a large amount of bubbles is produced. This stage, which corresponds to the initial linear part of the voltage-time curve (Figure1), is the traditional anodizing stage in which a thin porous film is formed.

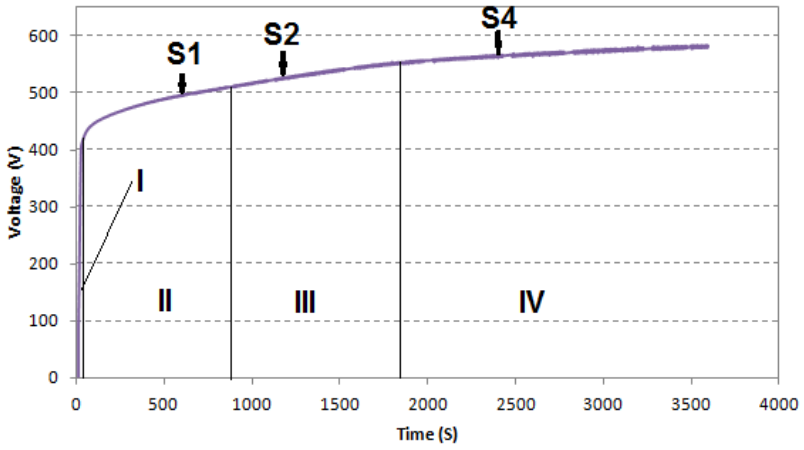

Figure 1- Voltage-time response for the PEO coated sample S6 (60 min).

When the voltage reaches a certain threshold, which is termed the 'break down voltage', dielectric breakdown occurs in some regions of the coating and the surface of the sample is covered by many fine and uniform sparks with a bluish white color. This creates many small uniform micro-pores [8]. In stage two, three, and four, which occur after the breakdown voltage is reached, the rate of voltage changes varies based on the process conditions applied. In a study [12] in which an electrolyte containing 2 g/L Na_2SiO_3 and 2 g/L KOH was used with similar

electrical conditions to the current study, the voltage-time response of the process showed a different behaviour with the four stages having different slopes, onset times, and durations. Stage II in the present study is more than twice as long as stage II in the abovementioned study. This shows how the electrolyte composition can affect the coating growth behavior during PEO.

2- Coating Thickness

Coating thickness measurements (Figure 2) revealed an increase in the coating thickness with deposition time. The average coating growth rate was about 0.95 µm/min. Optical microscope images showing the cross sections of the coated samples are presented in Figure 3. There are pores present in the coating which could be the result of gas entrapment in the molten coating during formation.

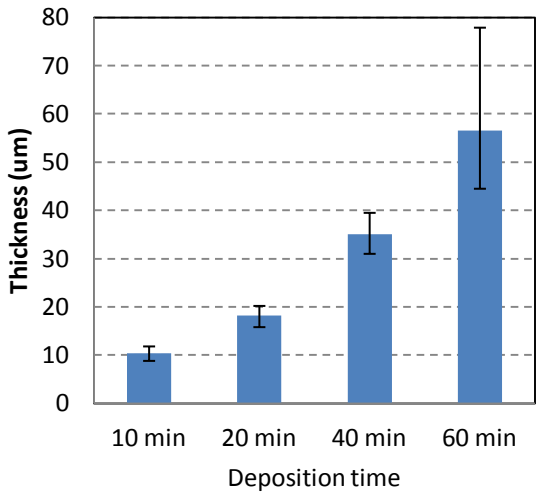

Figure 2- PEO coatings thickness variations with deposition time.

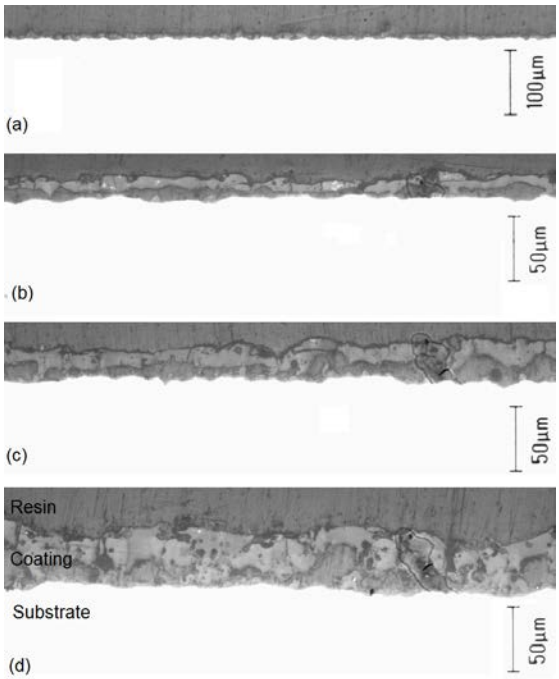

Figure 3- Optical microscope images showing cross sections of coatings on samples (a) S1, (b) S2, (c) S4, and (d) S6.

3- Coating Surface Morphology

Figure 4 illustrates the surface features of the PEO coated samples produced at different deposition times. Two different regions are observed on the surface of these samples: a nodular structure and a round, circular area. The circular area, which typically has a hole in the middle, is a discharge channel through which molten materials flow out to the surface from the substrate and coating interface [12]. In Figures 4-b to 4-c discharge channels can be observed as circular spots resembling craters. The craters are presented at a higher magnification with the point EDX analysis in Figure 5. As can be seen, the craters are rich in aluminum while the nodular structure is rich in Si. Discharge channels are always surrounded by craters [6, 13]. The oxide film growth is the result of the ejection and solidification of the molten oxide aluminum when it flows out through the discharge channels created due to the breakdown of the oxide layer [9].

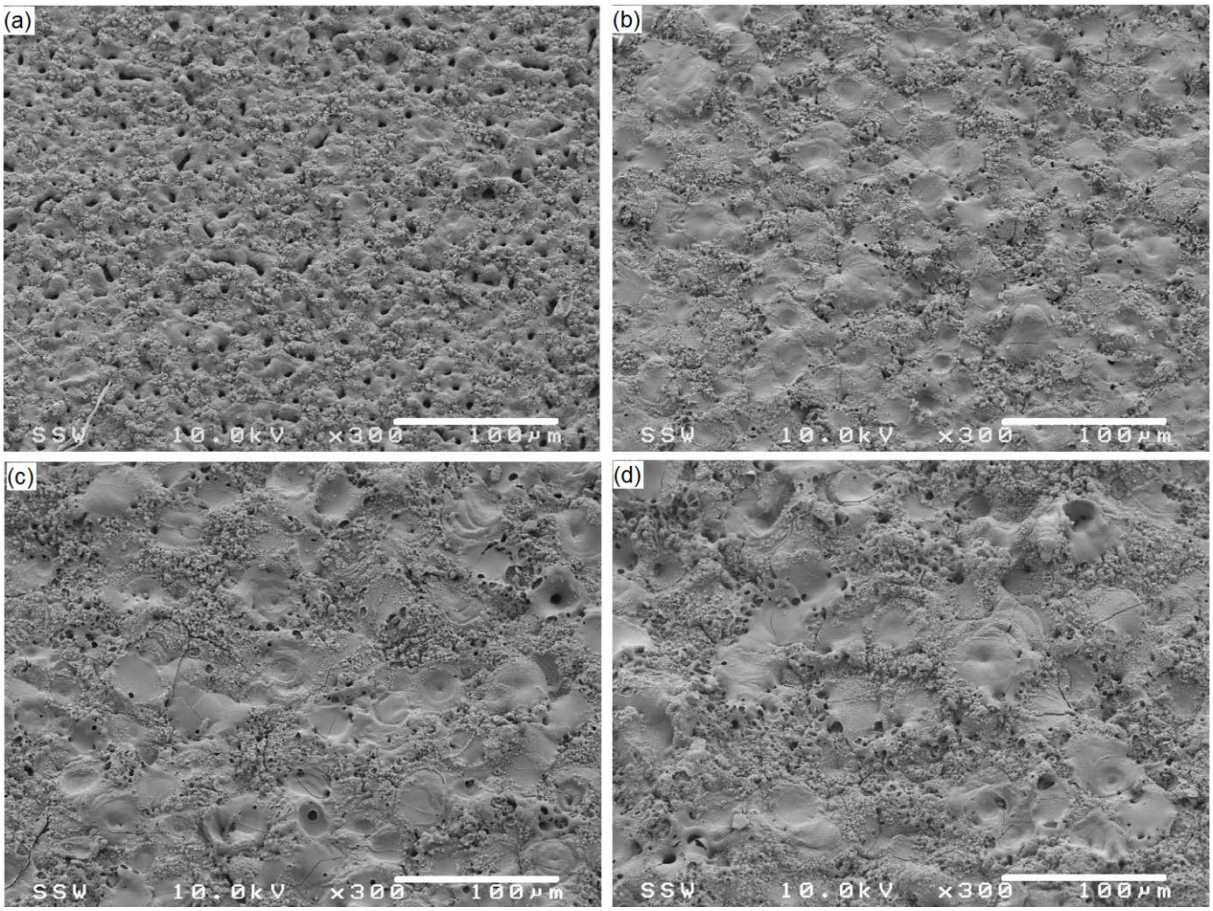

Figure 4- SEM micrographs of the free surfaces of samples, (a) S1, (b) S2, (c) S4, and (d) S6

Surface feature of sample S1 (Figure 4-a) is different from other samples. In sample S1, coated for 10 min, a nodular structure with many micro-pores are observed scattering across the surface area while samples coated for longer times (Figures 4-b, c, and d) exhibit nodular structures and craters with occasional micro-pores. Figure 1 shows that the deposition time for sample S1 falls in stage II, while for other samples deposition times were long enough to enter stage III and IV. Moreover, during the early stages of the coating process (first 10-12 min) the sparks appearing on the surface of the sample were small, bluish white in color and had a high spatial density. However, as the coating process proceeded, the color changed to yellow and then orange. From these observations it can be deduced that the coating growth behavior and sparking mechanisms change during different stages of the process. For the specific process conditions used in this study, a deposition time of 10 min produced many micro-pores on the surface of the coating which is not favorable.

4- Phase Analysis

Figure 6 illustrates the X-ray diffraction (XRD) spectra of the as deposited surface layers of PEO coatings processed for 10, 20, 40, and 60 min. To prevent the aluminum substrate peaks from masking the peaks belonging to phases present in the coating, glancing angle XRD operated at an

incident angle of 3.5° was used. It can be concluded from Figure 6 that the surface layers of the PEO coatings are mainly comprised of γ-Al_2O_3 for treatment times of 10 and 20 min. At longer treatment times (40 and 60 min) some mullite is also observed in addition to γ-Al_2O_3.

The extremely high cooling rates, when the molten alumina is ejected out and comes in contact with the electrolyte, favour the formation of γ-Al_2O_3 during solidification [9]. It was previously reported [10, 14, 15] that in Si containing electrolytes, the concentration of Si species is higher on the surface of the PEO coatings. It has been proposed [8, 16] that Si forms insoluble gels on the surface of PEO coatings. A conceptual model proposed by Dehnavi et al. [12] explains Si distribution on the surface of samples coated in electrolytes containing Si species. It was suggested that the ejection force of the micro-discharges formed on the surface of the coating detaches the Si rich species adsorbed on the coating. As the deposition time increases, micro-discharges become more intense while their numbers decrease. The lower spatial density of micro-discharges leaves more areas with Si rich species and this could enhance the formation of mullite ($3Al_2O_3.SiO_2$) at treatment times of 40 and 60 min where the number of micro-discharges decreased compared to deposition times of 10 and 20 min.

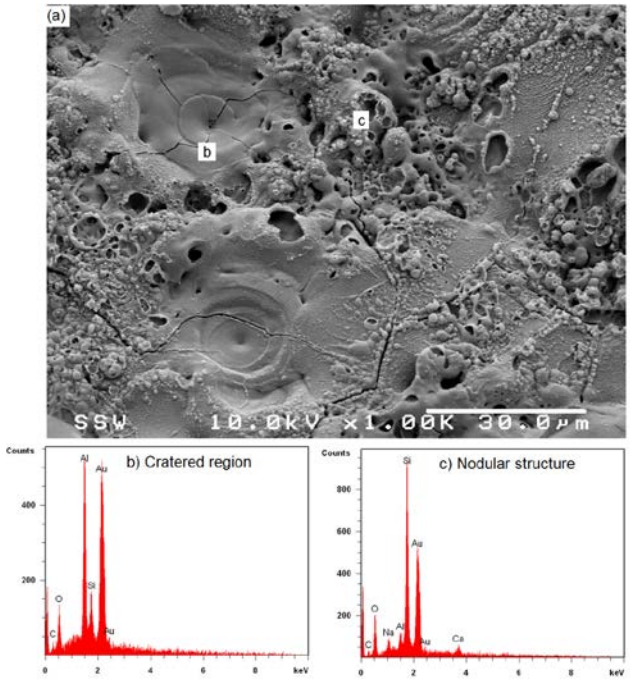

Figure 5- (a) SEM micrograph showing the coating surface morphology on sample S4; (b) and (c) EDX analysis from areas “b” and “c” respectively.

Conclusions

6061 aluminum substrates were PEO treated at different times. The results obtained from the characterization techniques show a clear correlation of the coatings microstructure with the voltage-time response of the process. It was concluded that the coating growth behavior and sparking mechanisms change during different stages of the process. The sample coated merely in stage II showed many micro-pores scattered across the surface area. In samples coated for

longer times, craters were observed on the coating surface which are characteristics of stages III and IV. The size of the craters increased while their spatial intensity decreased with deposition time. This suggests the importance of controlling processing conditions so that coatings are produced in the proper stage to have improved performances.

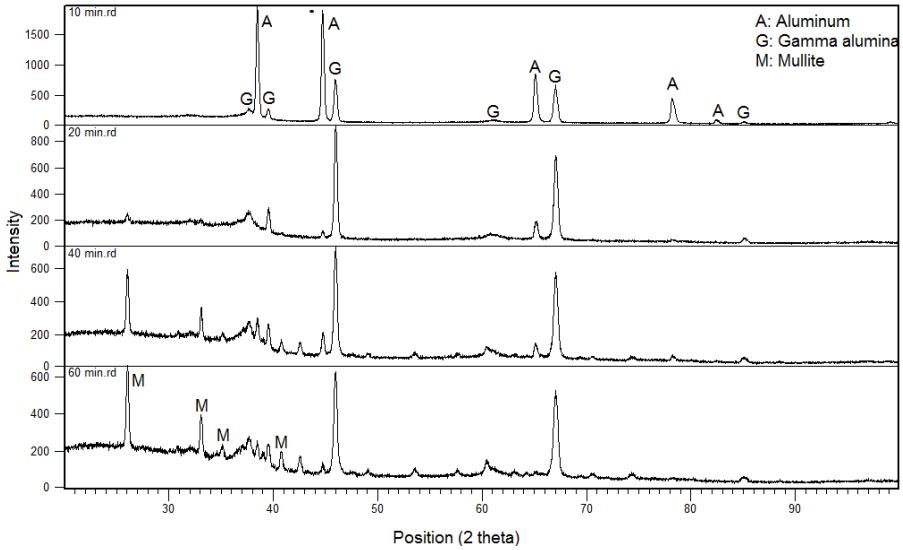

Figure 6- XRD spectra of PEO coatings processed for 10, 20, 40, and 60 min.

References

1. H. Li, R. Song, Z. Ji, "Effects of Nano-additive TiO_2 on Performance of Micro-arc Oxidation Coatings Formed on 6063 Aluminum Alloy," *Trans. Nonferrous Met. Soc. China 23 (2013) 406−41.*

2. M. M. Student, V. M. Dovhunyk, M. D. Klapkiv, V. M. Posuvailo, V. V. Shmyrko, and A. P. Kytsya, " Tribological Properties of Combined Metal-Oxide-Ceramic Layers on Light Alloys," , *Materials Science, 48 (2) (2012), 180-190.*

3. T. Abdulla, A. Yerokhin, R. Goodall, "Effect of Plasma Electrolytic Oxidation Coating on the Specific Strength of Open-cell Aluminium Foams," *Materials and Design 32 (2011), 3742–3749.*

4. J. Martin, A. Melhem, I. Shchedrina, T. Duchanoy, A. Nominé, G. Henrion, "Effects of Electrical Parameters on Plasma Electrolytic Oxidation of Aluminium," *Surf. Coat. Technol. 221 (2013) 70–76.*

5. A. L. Yerokhin, V. V. Lyubimov , R. V. Ashitkov, " Phase Formation in Ceramic Coatings During Plasma Electrolytic Oxidation of Aluminum Alloys," *Ceramics International 24 (1998), 1-6*

6. F. Mécuson, T. Czerwiec, G. Henrion, T. Belmonte, L. Dujardin, A. Viola, J. Beauvir, "Tailored Aluminium Oxide Layers by Bipolar Current Adjustment in the Plasma Electrolytic Oxidation (PEO) Process," *Surf. Coat. Technol. 201 (21) (2007) 8677.*

7. A.L. Yerokhin, A.A. Voevodin, V.V. Lyubimov, J. Zabinski, M. Donley, "Plasma Electrolytic Fabrication of Oxide Ceramic Surface Layers for Tribotechnical Purposes on Aluminium Alloys," *Surf. Coat. Technol. 110 (1998) 140–146.*

8. B. L. Jiang, Y. M. Wang, "Plasma Electrolytic Oxidation Treatment of Aluminum and Titanium Alloys," *Surface Engineering of Light Alloys: Aluminum, Magnesium and Titanium Alloys*, H. Dong, ed. (CRC Press, 2010), 110-153.
9. A130] G. Sundararajan, L. Rama Krishna," Mechanisms Underlying the Formation of Thick Alumina Coatings through the MAO Coating Technology," *Surf. Coat. Technol. 167 (2-3) (2003) 269-276.*

10. S. Moon, Y. Jeong, "Generation Mechanism of Microdischarges During Plasma Electrolytic Oxidation of Al in Aqueous Solutions," *Corros. Sci. 51 (7) (2009) 1506-1512.*

11. R. O. Hussein, X Nie, D. O. Northwood, A. L. Yerokhin and A Matthews, "Spectroscopic Study of Electrolytic Plasma and Discharging Behaviour During the Plasma Electrolytic Oxidation (PEO) Process," *J. Phys. D: Appl. Phys. 43 (2010) 105203*-105216.

12. V. Dehnavi, B. L. Luan, D. W. Shoesmith, X. Y. Liu, S. Rohani, "Effect of Duty Cycle and Applied Current Frequency on Plasma Electrolytic Oxidation (PEO) Coating Growth Behavior," *Surf. Coat. Technol. 226 (2013) 100–107*

13. L. Rama Krishna, K.R.C. Somaraju, G. Sundararajan, "The Tribological Performance of Ultra-hard Ceramic Composite Coatings Obtained Through Microarc Oxidation," *Surf. Coat. Technol. 163–164 (0) (2003) 484-490.*

14. F. Monfort, A. Berkani, E. Matykina, P. Skeldon, G.E. Thompson, H. Habazaki, K. Shimizu, "A Tracer Study of Oxide Growth during Spark Anodizing of Aluminum," *J. Electrochem. Soc. 152 (6) (2005) 382-387.*

15. F. Monfort, E. Matykina, A. Berkani, P. Skeldon, G.E. Thompson, H. Habazaki, K. Shimizu, "Species Separation During Coating Growth on Aluminium by Spark Anodizing," *Surf. Coat. Technol. 201 (21) (2007) 8671-8676.*

16. F. Monfort, A. Berkani, E. Matykina, P. Skeldon, G.E. Thompson, H. Habazaki, K. Shimizu, "Development of Anodic Coatings on Aluminium under Sparking Conditions in Silicate Electrolyte" *Corros. Sci. 49 (2) (2007) 672-693.*